Available online at www.sciencedirect.com
ScienceDirect
Electrochimica Acta 52 (2007) 3607–3614
ELECTROCHIMICA Acta
www.elsevier.com/locate/electacta

Water flooding and pressure drop characteristics in flow channels of proton exchange membrane fuel cells

Xuan Liu, Hang Guo *, Fang Ye, Chong Fang Ma

Key Laboratory of Enhanced Heat Transfer and Energy Conservation, Ministry of Education, College of Environmental and Energy Engineering, Beijing University of Technology, 100 Pingleyuan, Chaoyang District, Beijing 100022, PR China

Received 24 July 2006; received in revised form 4 October 2006; accepted 11 October 2006
Available online 28 November 2006

Abstract

Water flooding of the flow channels is one of the critical issues to the design and operation of proton exchange membrane fuel cells (PEMFCs). The liquid water and total pressure drop characteristics both in the anode and cathode parallel flow channels of an operating PEMFC were experimentally studied. The gas/liquid two-phase flow both in the anode and cathode flow channels was observed, and the total pressure drop between the inlet and outlet of the flow field was measured. The effects of cell temperature, current density and operating time on the total pressure drop were investigated. The results indicated that the total pressure drop in the flow channels mainly depends on the resistance of the liquid water in the flow channels to the gas flow, and the different flow patterns distinguish the total pressure drops in the flow field. Clogging by water columns result in a higher pressure drop in the flow channels. The total pressure drop measurement can be considered as an in situ diagnoses method to characterize the degree of the flow channels flooding. The liquid water in the cathode flow channels was much more than that in the anode flow channels. The pressure drop in the cathode flow channels was higher than that in the anode flow channels. During the fuel cell operation, the cell performance decreased gradually and the pressure drop both in the anode and the cathode flow channels increased. The rate of flooding at the cathode side reached 49.56% under experimental conditions after 78 min of operation. However, it was zero at the anode side.

Keywords: Proton exchange membrane fuel cells; Flow channels flooding; Pressure drop; Condensation; Visualization

1. Introduction

In proton exchange membrane fuel cells (PEMFCs), the direct conversion of the chemical energy of reactants to electrical energy is achieved with high efficiency and good environmental compatibility [1–3]. The overall behavior of PEMFCs can be described by the performance curves, which reveal the dependence of cell voltages on the operating current density. Such a characteristic curve is a conclusion of the interplay among all the transport and electrochemical processes that take place inside PEMFCs. Since the dominant mechanism for the performance of a PEMFC may shift from one to another regime, different types of behavior are observed at different regimes of operating current densities. Most of the previous works focused on the electrochemical aspects to enhance cell performance and reduce cell costs. The improvements and optimizations discussed in those previous works include: exploring more active electrocatalysts, optimization membrane electrode assembly structures, modifying and searching for alternative membrane materials, and reduction of the catalyst loading [4–9].

At present, more and more research focus on the understanding of the thermodynamic phenomena and on the fluid mechanisms coupled with the electrochemical processes within PEMFCs [10–13]. In order to improve fuel cell design and operation, it is necessary to learn more about the mechanisms that cause the performance losses; for example, the losses due to mass transfer limitation and fluid dynamic characteristics [14–17]. The issues of the fluid dynamics are needed to be studied experimentally for model validation [18–21].

In PEMFCs, air or oxygen as oxidant and hydrogen as fuel are supplied. At the anode, hydrogen is consumed; while the electrons transport to the cathode via an external circuit and the hydrogen ions (protons) transport to the cathode through the polymer electrolyte membrane. It should be noted that, the H^+ transfer can be realized only when the membrane is strongly hydrated.

* Corresponding author. Tel.: +86 10 67391612x8311; fax: +86 10 67392774.
E-mail address: hangguo@sohu.com (H. Guo).

0013-4686/$ – see front matter © 2006 Elsevier Ltd. All rights reserved.
doi:10.1016/j.electacta.2006.10.030

The electrochemical reactions involved are:

$$H_2 \rightarrow 2H^+ + 2e^- \quad \text{(anode)}$$

$$2H^+ + \tfrac{1}{2}O_2 + 2e^- \rightarrow H_2O \quad \text{(cathode)}$$

$$H_2 + \tfrac{1}{2}O_2 \rightarrow H_2O \quad \text{(overall)}$$

A significant technical challenge in a PEMFC is that the fuel cell is prone to excess liquid water formation due to water production from the oxygen reduction reaction at the cathode. Liquid water may fill the pores of the gas diffusion layer (GDL), and block the transport of oxygen into the catalyst layer (CL), and may further cover the catalyst sites. This is known as "GDL/CL flooding". If liquid water accumulation becomes excessive in a PEMFC, water columns or water bands may form inside the flow channels, thereby blocking or clogging the gas flow. This condition is referred to as "flow channel flooding".

Visualization has the advantage of in situ observation to study the water flooding or fluid dynamics in the flow channels of PEMFCs. Tüber et al. [22] studied the visualization of liquid water buildup in the cathode channels of a transparent PEMFC operating at room temperature. They presented the images of the effect of operating time on the water flooding and cell performance in a constant voltage operation mode. The effects of the air stoichiometry, temperature, air humidity and different characteristics of diffusion layers were discussed. The influence of hydrophobic and hydrophilic diffusion layers compared to standard carbon papers on water transport was investigated. Yang et al. [23] visually studied the mechanics of the liquid water transport on a GDL surface under automotive conditions, including emergence as droplets at preferential locations, droplet coalescence, droplet detachment by the gas core flow, and droplet wicking onto hydrophilic channel walls. The results showed that an annular film flow of liquid water turned into a water lens due to the instability of thick films. Zhang et al. [24] studied experimentally and theoretically the liquid water transport and removal from the gas diffusion layer (GDL) and gas channel of a polymer electrolyte fuel cell. In situ observations of the liquid water distribution on the GDL surface and inside the gas channel were made. The liquid droplet formation and emergence from the GDL surface were also characterized and two modes of liquid water removal from the GDL surface were identified. Wang [25] summarized the current status of fundamental models for fuel cell engineering and indicated where this burgeoning field is heading by a review. The review presented a systematic framework for fuel cell modeling research and reviewed the work performed in the past decade on PEMFCs, DMFCs, and SOFCs, respectively. In particular, the review summarized the liquid water transport within PEMFCs and presented the image of liquid water droplets on GDL of different wettability. The recent techniques and results of two-phase flow visualization of PEMFCs were also presented. Liu et al. [26] experimentally studied the water flooding and two-phase flow of reactants and products in the cathode flow channels of an operating transparent PEMFC. Three different flow fields including parallel flow field, interdigitated flow field and cascade flow field were adopted. The effects of flow field type, cell temperature, cathode gas flow rate and operation time on water build-up and cell performance were studied. Experimental results indicated that the liquid water columns accumulating in the cathode flow channels can reduce the effective electrochemical reaction area and shut down mass transport, resulting in cell performance loss. The evolution of liquid water removal out of channels was also recorded by a high-speed video.

These works reported the liquid water in the cathode flow channels. However, at the anode side, the liquid water also appears in typical conditions of low temperatures or low gas flow rates. Although no water is produced electrochemically at the anode side, the water at the cathode side can penetrate through the membrane and reach the anode side. When the fuel cell is operated in a steady state, water molecules in the fuel cell are driven by three mechanisms: an electro-osmotic drag due to potential difference, a back diffusion due to the concentration gradient, and the pressure difference between the cathode and anode [27,28]. The direction of the back diffusion is always from the cathode to the anode. If the water that is removed from the anode is less than the water that comes from the cathode, the water accumulates and the flooding may appear.

In addition, the characteristics of the total pressure drop in the flow field have a significant effect on the fuel cell system power consumption. The behavior of the pressure drop in PEMFCs is complex because the cell is prone to flooding due to excess liquid water formation. The emergence of the water droplets or water columns in the flow channels influences the gas flow, sometimes shutting it down, which makes the pressure drop behavior in the flow channels different from the single-phase gas flow. Also, the pressure drop measurement can be considered as an in situ diagnoses method to characterize the degree of the flow channels flooding. Until now, studies on the pressure drop behavior in the fuel cell flow field are quite scarce. Argyropoulos et al. [29,30] and Yang et al. [31] studied and reported the pressure drop behavior in the anode flow field of DMFCs. Maharudrayya et al. [32] studied the pressure drop and flow distribution in multiple parallel channel configurations used in PEMFC stacks. They developed the algorithms to calculate flow distribution and pressure drop in multiple U- and Z-type flow configurations. The results were validated by comparison with the data that was obtained from three-dimensional computational fluid dynamics (CFD) simulations.

In this paper, the visualization of the liquid water (flooding) both in the anode and cathode flow channels of an operating PEMFC was conducted. The total pressure drop between the inlet and outlet of a PEMFC both in the anode and cathode flow channels were measured. The effects of the cell temperatures, current density and operating time on the total pressure drop were studied.

2. Experimental

2.1. Transparent PEMFCs

In order to observe the gas liquid two-phase flow inside PEMFCs, a PEMFC with a transparent window was used in

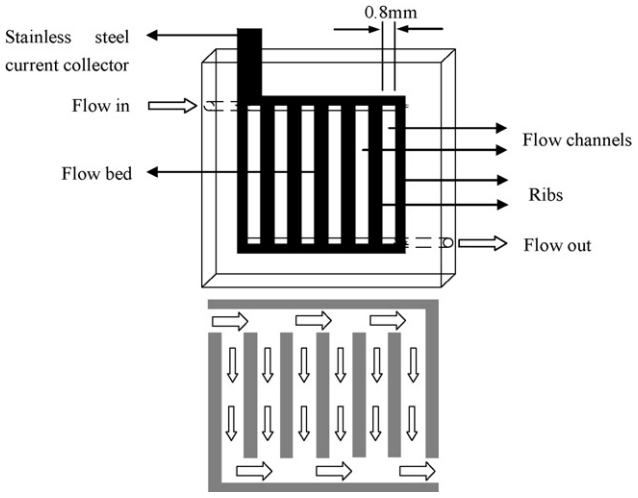

Fig. 1. Schematics and diagrams of the transparent PEMFC.

this research. Fig. 1 shows the schematics of the transparent PEMFC and the diagrams of the gas flow passages. A gold coated stainless steel plate was used as the flow field and current collector. Plexiglass was the transparent material outside the flow field. The thickness of the stainless steel was 1 mm and there were nine slots of 0.8 mm width and 22.4 mm length in it. Therefore, when the stainless steel was installed between the transparent plexiglass and membrane electrode assembly (MEA), the flow channels were formed (1 mm in depth). The total effective area of flow field was 5 cm^2. Teflon coated glass fiber cloths with slots matching the slots in the stainless steel were sandwiched between the flow field and the plexiglass as the sealing strip. Two main channels as the manifolds, flow in and flow out, in the transparent plexiglass connected the channels of the fuel cell flow field and the pipelines of the experimental system. Another two stainless steel end plates were used for clamping. A window was set up in the end plate so that the liquid water and flow behaviors inside the PEMFC were directly observable. An electrical heater was used to heat the fuel cell. A unit temperature controller including electromagnetic relay and temperature sensor (PT100) was used to control the cell temperature.

MEAs of 5 cm^2 active area made by Fuyuan Century Fuel Cell Power Co. Ltd. were used for this study. The MEA was composed of a Nafion 1135 membrane that was sandwiched between two carbon papers. Both the anode and the cathode were loaded with platinum of 0.4 mg/cm^2. As pointed out by Lu and Wang [13], and Yang et al. [23], the surface characteristics of the gas diffusion layer (GDL) influences the liquid water distribution, for example the interfacial liquid water coverage. The main difference between a hydrophilic and a hydrophobic GDL lies in the liquid water behavior at the GDL interface. The former tends to spread the liquid water and hence gets a much higher coverage at the interface, however, the latter forms discrete droplets and features a much lower surface coverage by the liquid water. The contact angle of a water droplet on the GDL used in this paper was measured by a contact angle instruments (First Ten Angstroms, FTA 100) before the experiment, as shown in Fig. 2. Obviously a hydrophobic GDL shows the feature of easier water droplets removal.

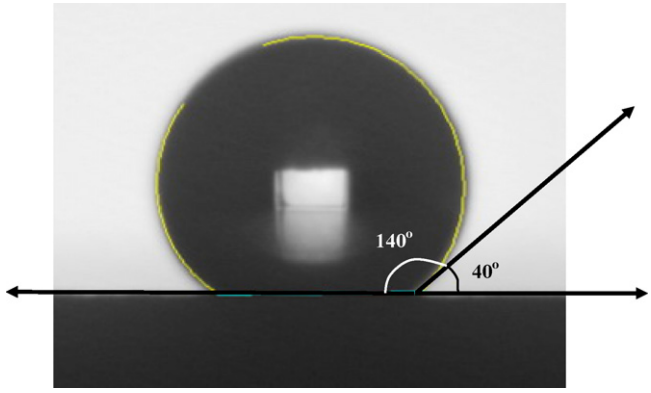

Fig. 2. Contact angle of the hydrophobic GDL used in this study.

2.2. Experimental set-up

The experimental set-up consists of: (i) a fuel and oxidant reactant supply system; (ii) a cell performances test system; (iii) a high-speed video and digital camera recording system; (iv) a data collector and analysis system.

Pure hydrogen and oxygen were used, respectively, as the fuel and the oxidant reactant. The gases to the fuel cells were not humidified, and the fuel cell was sealed, so all the water observed in the flow channels of the transparent fuel cells was generated from the electrochemical reaction only. Gas flow rates were quantified by the mass flow controllers (MFCs, Type SY 9312B-EX) with a precision of 0.5%. Gas pressures and pressure drops between the inlet and the outlet of the flow channels were measured by pressure sensors (Type WQSBP) with a precision of 0.1%, and pressure difference sensors (Type 1151DP) with a precision of 0.1%, respectively. A nitrogen purge system made sure to clean the fuel and oxidant reactant left in the test system pipelines and fuel cells. An electronic load (Arbin FCTS LNR) was applied in the external circuit of the tested fuel cell. The images of gas liquid two-phase flow both in the anode and cathode flow channels were recorded by a digital camera (Sony, DSC-F505V).

2.3. Configuration and data correction

The experiments were performed when the flow channels of the fuel cell was orientated vertically. The flow field was arranged as shown in Fig. 1. Hydrogen was supplied as the fuel into the anode flow field from the upper left corner, and oxygen was supplied as the oxidant into the cathode flow field from the upper right corner.

For the present vertical fuel cell flow field, as shown in Fig. 1, the total pressure drop can be expressed by the following equations:

$$\Delta P_T = \Delta P_m - \Delta P_G \quad (1)$$

where ΔP_T is the total pressure drop in the flow field, ΔP_m represents the measured pressure drops by the differential pressure sensors, ΔP_G is the gravitational term, which can be calculated as ρgh and denotes the hydraulic head caused by the altitude difference. In this gravitational term, ρ represents the density of the liquid water in the flow channels, g represents the acceleration of gravity as a constant value of 9.8 m/s^2, and h represents the height of the water columns based at the outlet. The variable of h could be measured in the photographs.

Eq. (1) implies that the total pressure loss in the flow channels will be obtained by subtracting the gravitational pressure drop from the measured pressure drop. The total pressure loss, ΔP_T, depends mainly on the resistances of the liquid phase to the gas flow. All results in the present work were corrected according to Eq. (1).

3. Results and discussion

3.1. Pressure drop in PEMFCs

Fig. 3 shows the cell performance and pressure drop characteristics at temperatures of 35 °C and 75 °C, respectively. The oxygen and hydrogen were supplied at the flow rates of 69.6 ml/min and 139.3 ml/min, respectively, and an ambient pressure at the outlet. The results show that the pressure drop both in the anode and cathode flow channels increased with the elevation of the current density. In PEMFCs, the total pressure drop in the flow channels varies because of two-phase flow dynamics, which relates to the flow channels flooding. Some of the water droplets coalesce to form water columns, clogging or shutting down the gas flow. The water production from the oxygen reduction reaction is based on the operating current density according to the Faraday's law. The higher the current density, the more water is produced [33]. The liquid water droplets

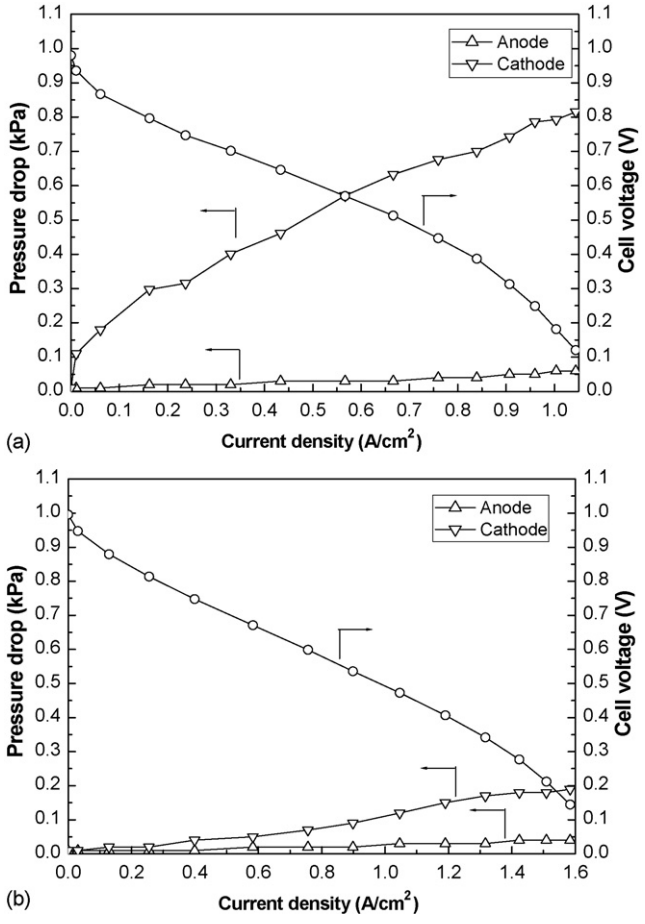

Fig. 3. Cell performance and pressure drop characteristics. (a) 35 °C and (b) 75 °C.

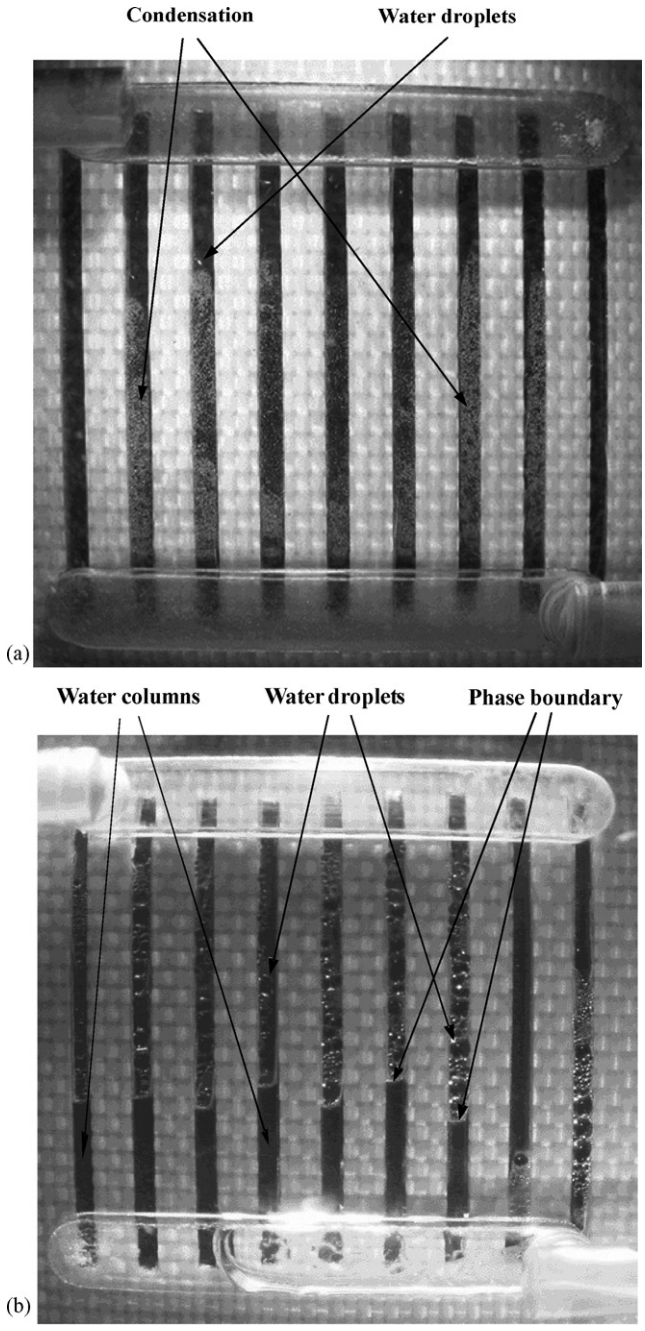

Fig. 4. The visualization of liquid water in the anode and cathode flow channels at 35 °C. (a) The liquid water in the anode flow channels and (b) the liquid water in the cathode flow channels.

emerge in the flow channels under conditions of oversaturation of water vapor in the gas phase. At a higher current density, the liquid water in the flow channels is more than that at a lower current density. The water accumulation in the flow channels formed water columns and blocked the gas flow, therefore, the pressure drop increased in the flow channels when the liquid water appeared.

In Fig. 4, the liquid water in the flow channels of the transparent PEMFC with the parallel flow channels at 35 °C is shown. Photo (a) shows the image of liquid water in the anode flow channels, and photo (b) shows the image of liquid water in the cathode flow channels. The photos were taken after the fuel cell had operated at a constant current of 2 A (0.4 A/cm^2) for 5 min. During the evolution of liquid water in the flow channels, condensation plays an important role in the emergence of flooding. Fog was firstly visible on the inner surface of the transparent material in the static state operation. It can be seen that the fog consisted of very small water droplets condensed on the inner surface of the transparent material. Then, the water droplets increased in size, and some water droplets were able to grow to a size of 0.7–0.8 mm in diameter, comparable to the cross-sectional dimension of the flow channels. Finally, the water droplets accumulated in the flow channels and water columns appeared in the flow channels. The water at the anode side was caused by diffusing through membrane from the cathode side due to a high water concentration gradient. In our experiments, only fog was observed in the anode flow field. This is because there was not enough water condensation to generate bigger water droplets. As can be seen from the photos, the water flooding in the cathode flow channels was more serious than that in the anode flow channels and the flooding area in the cathode flow field was more than that in the anode flow field. This fact explains why the total pressure drops in the cathode flow channels is much more than the total pressure drops in the anode flow channels.

As can be seen from Fig. 4, the water distribution in whole flow field was non-uniform, and most of the liquid water appeared at the downstream section of the flow field. This means that the liquid water will not appear before the water vapor reaches saturation in the gas phase. It seems that the non-uniform water distribution and the non-uniform current distribution are coupled, and [23] showed that the upstream section where fewer liquid water appeared, produced higher current densities. When the flow channels are filled with liquid water, the gas can hardly reach the electrochemical reaction sites.

3.2. Effect of the cell temperature on pressure drop

Fig. 5 shows the liquid water of the flow channels in the transparent PEMFC with parallel flow channels at 75 °C. The photos display that at a higher cell temperature of 75 °C, the liquid phase region can be reduced compared to the condition of 35 °C. This is because the evaporation rate of water increases with temperature elevation. It caused higher saturated vapor pressure of water. It has been known that the occurrence of liquid water requires an oversaturated gas flow. The liquid water would not appear when the saturated vapor pressure of water is higher than the partial pressure of water in the oxygen [22]. As can be seen from Fig. 5, at higher temperatures, the liquid phase region became smaller.

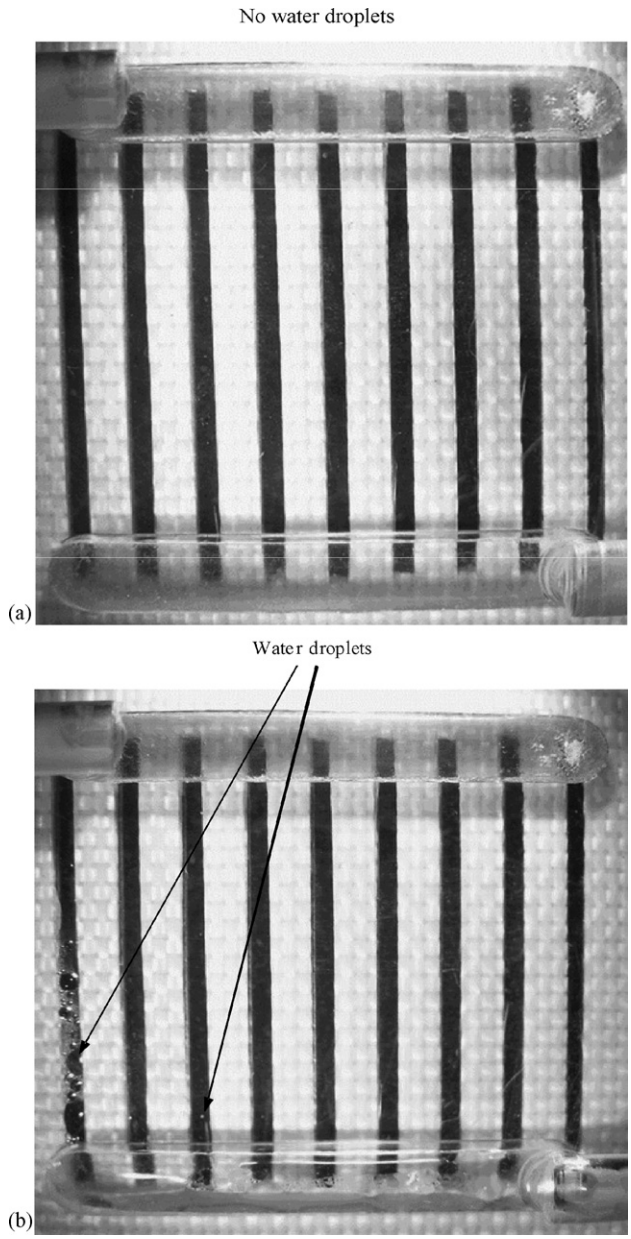

Fig. 5. The visualization of liquid water in the anode and cathode flow channels at 75 °C. (a) No liquid water in the anode flow channels and (b) the liquid water in the cathode flow channels.

Fig. 6 shows the effect of the cell temperature on the total pressure drop when the fuel cell operated at different temperatures. The total pressure drops both in the anode flow channels and in the cathode flow channels decreased with the cell temperature elevation because the resistance of the liquid phase to the gas flow became smaller. And it was also found that in the cathode flow channels, the total pressure drop decreased dramatically but it decreased a little in the anode flow channels during the cell temperature increase. This fact is attributed to the decrease of the resistance of the liquid phase to the gas flow because there is

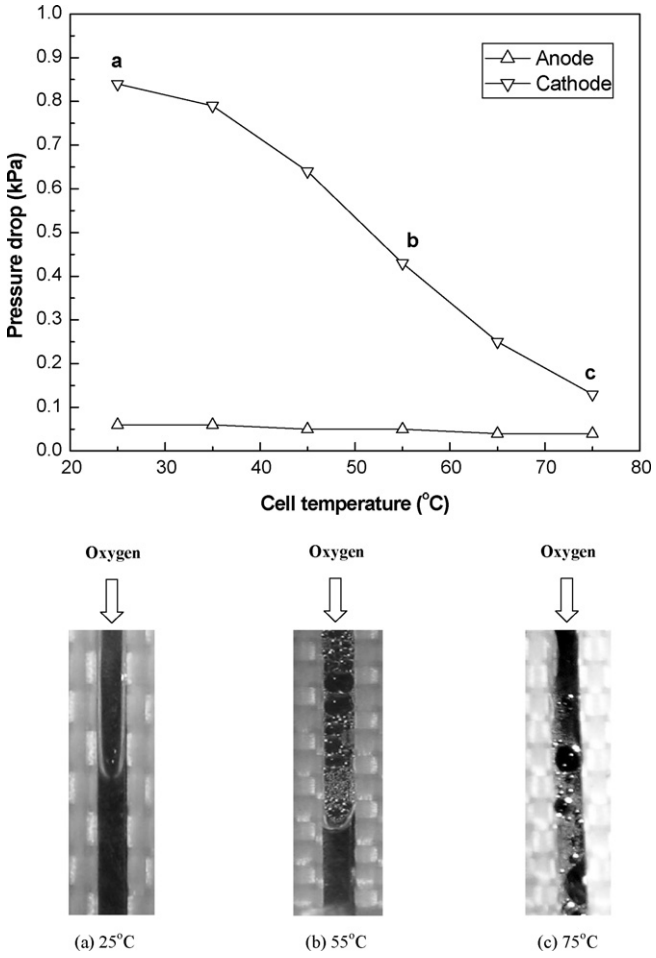

Fig. 6. Effect of cell temperature on the total pressure drop.

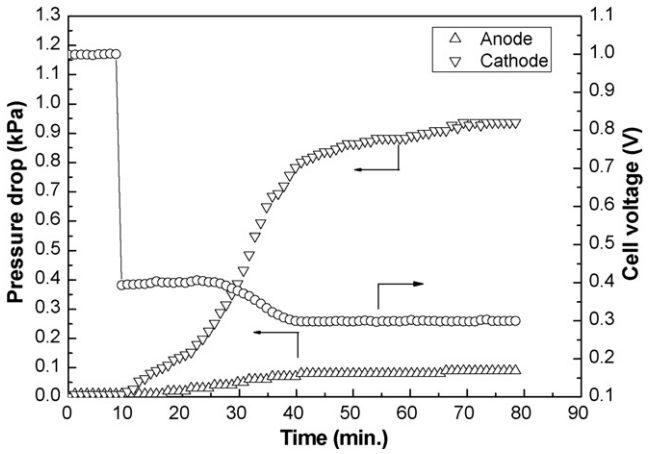

Fig. 7. Effect of operating time on total pressure drop.

little liquid water condensation in the flow field when the temperature is elevated. At a low temperature of 25 °C, the water condensation accumulated in the cathode flow channels forming water columns. The water columns clogged the flow channels and shut down the gas flow. A clear phase boundary was found in Fig. 6, photo (a), and the water columns moved very slowly with the gas flow. The water columns clogging results in the highest pressure drop in the flow channels. At a higher temperature of 55 °C (Fig. 6, photo (b)), less water vapor condensed into liquid water. The gas phase region expanded and the water column became shorter. As a result, the total pressure drop decreased. When the temperature was increased further to 75 °C (Fig. 6, photo (c)), most of the water vapor was removed out of the flow channels with the gas flow without condensation. The sizes of water droplets were not big enough to coalesce. At this situation, discrete water droplets were distributed in the flow channel. Because of the water droplets on the inner surface of the transparent material, we could not observe whether or not there were water droplets in the main flow region. Because the resistance of the water droplets to the gas flow is much less than the resistance of the water columns to the gas flow, the total pressure drop under this situation was lowest in this experiment. The three photos discussed above were the visualization results in the cathode flow channels. As can be seen, in the anode flow channels, only fog was observed on the inner surface of the transparent material, and a liquid column could not be found.

3.3. Effect of the operating time on pressure drop

The effect of the operating time on the total pressure drops in both the anode and the cathode flow channels was shown in Fig. 7. The fuel cell operated at a constant temperature of 25 °C, atmospheric pressure conditions and the oxygen and hydrogen were supplied at the flow rates of 69.6 ml/min and 139.3 ml/min, respectively. The water generation continued under operating conditions, and the water accumulated in the flow channels, forming the water columns and shutting down the gas flow. The liquid water accumulation in the flow field made the cell voltage decreased and the total pressure drops in both the anode and the cathode flow channels increased under operating condition. As can be seen from Fig. 7, before 8.5 min, the cell voltage and pressure drop kept a constant value due to no water production when the fuel cell operated under open circuit condition. When the fuel cell was loaded at constant current of 2 A at 8.5 min, the cell voltage dropped suddenly, and a rapid drop of cell performance could be observed. This is the result of electrochemical reaction and mass transfer in fuel cells. Similar drastic declines of cell performance were also reported and discussed by other researchers [22,23,26].

Fig. 7 shows that, the pressure drop in the anode flow channels increased from 0.01 kPa to 0.09 kPa, and the pressure drop in the cathode flow channels increased from 0.01 kPa to 0.936 kPa. The results imply that the total pressure drop is primary in the flow channels because of the resistance of the liquid water blockage to the gas flow in channels. Based on the results above, the different flow patterns distinguish the total pressure drops in the flow field, so the pressure drop measurement can be considered as an in situ diagnoses method to characterize the degree of the flow channels flooding. The data of the total pressure drops can feature the degree of water flooding in the flow channels of an operating PEMFC.

Fig. 7 also shows that because of the appearance of liquid water, after 25 min, the cell performance decreased gradually, and it finally reached a new steady state after about 40 min oper-

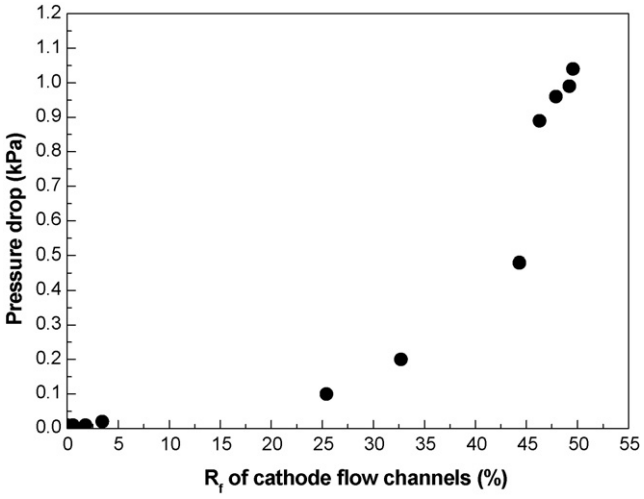

Fig. 8. Effect of cathode flooding rate on the total pressure drop.

ation. The total pressure drop became constant and reached a steady condition after about 70 min operation. This is attributed to the fact that the electrochemical processes are faster than the thermophysical processes, such as diffusion, mass transport, and fluid flow. The experimental results indicated that the thermophysical processes have great impact on fuel cell performance.

Fig. 8 shows the relationship of the rate of the flooding and the total pressure drop in the flow channels. The rate of the flooding was denoted as R_f (%) in this paper, which was the ratio of the length of the water columns in the flow channels, L_w, to the length of the flow channels, L_{ch}:

$$R_f = \frac{L_w}{L_{ch}} \quad (2)$$

Since both the length of the water columns L_w and the length of the flow channels L_{ch} can be measured in every photo, the ratio of R_f can be obtained. Fig. 8 shows the R_f of the cathode flow field reached 49.56% under our experiment conditions after 78 min of operation, and the cathode pressure drop increased with the R_f increase. Although some little water droplets in the anode flow channels can be found in the photo (Fig. 4(a)), the water columns were not found in the anode flow channels, so the R_f of the anode was regarded as zero in this experiment. Therefore, effect of R_f of the anode side on the anode pressure drop was not discussed. Fig. 9 shows the pressure drop in the flow channels and the rate of flooding (R_f) varied with the operating time. At the cathode side, the rate of flooding (R_f) increased dramatically with the operating time, and reached a plateau after about 30 min. At the anode side, however, the pressure drop increased a little with the operating time due to only the emergence of some little liquid water droplets, and the rate of flooding (R_f) was reported as zero because no water columns were found in the anode flow channels. The results indicated that the total pressure drop in the flow channels mainly depends on the liquid water in the flow channels, and the pressure drop in the cathode flow channels is primary in the total pressure drop of a PEMFC.

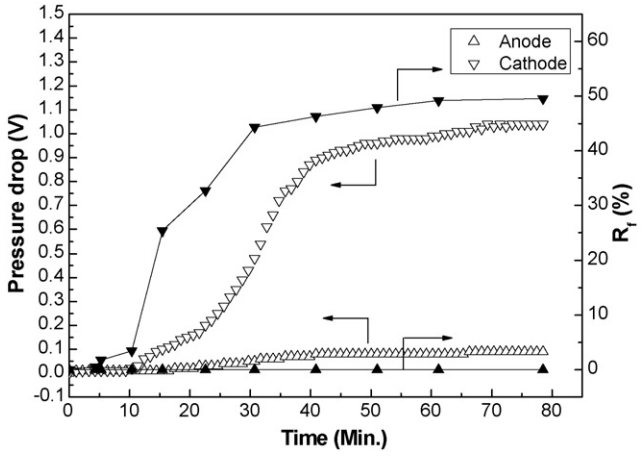

Fig. 9. Variation of rate of flooding and pressure drop.

4. Conclusion

The investigation of pressure drop characteristics and visualization study of liquid water both in the anode and cathode flow channels of an operating PEMFC consisting of parallel flow channels were conducted.

(1) The experimental results demonstrate that the water production at the cathode side can be driven to the anode side by the effect of diffusion due to the concentration gradient. The accumulation of the liquid water in channels has a significant influence on the cell performance due to the limitation of the mass transfer.

(2) The total pressure drop in the flow channels mainly depends on the resistance of the liquid water to the gas flow in the flow channels. The appearance of water columns results in a higher pressure drop in the flow channels.

(3) The total pressure drop increased with the increase of the current density, however, the total pressure drop decreased with increasing the cell temperature. During the fuel cell operation, the cell performance decreases gradually and the pressure drop both in the anode and the cathode flow channels increases. The total pressure drop in the cathode flow channels was higher than that in the anode flow channels.

(4) At the cathode side, the pressure drop and the rate of flooding (R_f) of cathode could finally reach a plateau and became constant.

Acknowledgments

This work is supported by the National Natural Science Foundation of China (Grant No.: 50406010, 50236010). The authors would like to acknowledge Dr. Maohai Wang for kindly help and discussion and Peter King P. Eng for editing.

References

[1] T. Susai, A. Hamada, J. Power Sources 92 (2001) 131.
[2] R.Z. Jiang, D. Chu, J. Power Sources 92 (2001) 193.
[3] S.G. Chalk, J.A. Milliken, J.F. Miller, J. Power Sources 71 (1998) 26.
[4] S. Ye, A.K. Vijh, L.H. Dao, J. Electrochem. Soc. 143 (1992) 7.

[5] G. Faubert, R. Côté, J.P. Dodelet, M. Lefèvre, P. Bertrand, Electrochim Acta 44 (1999) 2589.
[6] E.H. Yu, K. Scott, Electrochem. Commun. 6 (2004) 361.
[7] R. Ramkumar, S. Dheenadayalan, R. Pattabiraman, J. Power Sources 69 (1997) 75.
[8] M. Neergat, A.K. Shukla, J. Power Sources 104 (2002) 289.
[9] S.C. Thomas, X. Ren, S. Gottesfeld, P. Zelenay, Electrochim. Acta 47 (2002) 3741.
[10] H. Guo, C.F. Ma, M.H. Wang, J. Yu, X. Liu, F. Ye, C.Y. S Wang, Proceedings of First International Conference on Fuel Cell Science Engineering and Technology, ASME, Rochester, NY, April 21–23, 2003, p. 471.
[11] P. Argyropoulos, K. Scott, W.M. Taama, Electrochim. Acta 44 (1999) 3575.
[12] A. Hakenjos, H. Muenter, U. Wittstadt, C. Hebling, J. Power Sources 131 (2004) 213.
[13] G.Q. Lu, C.Y. Wang, J. Power Sources 134 (2004) 33.
[14] S. Um, C.Y. Wang, K.S. Chen, J. Electrochem. Soc. 147 (12) (2000) 4485.
[15] Z.H. Wang, C.Y. Wang, K.S. Chen, J. Power Sources 94 (2001) 40.
[16] J.J. Baschuk, X. Li, J. Power Sources 86 (2000) 181.
[17] L. You, H. Liu, Int. J. Heat Mass Transf. 45 (2002) 2277.
[18] M.M. Mench, Q.L. Dong, C.Y. Wang, J. Power Sources 124 (2003) 90.
[19] A. Parthasarathy, S. Srinivasan, A.J. Appleby, C. Martin, J. Electrochem. Soc. 139 (1992) 2856.
[20] R. Mosdale, S. Srinivasan, Electrochim. Acta 40 (1995) 413.
[21] F.A. Uribe, S. Gottesfeld, T.A. Zawodzinski, J. Electrochem. Soc. 149 (2002) A293.
[22] K. Tüber, D. Pócza, C. Hebling, J. Power Sources 124 (2003) 403.
[23] X.G. Yang, F.Y. Zhang, A.L. Lubawy, C.Y. Wang, Electrochem. Solid-State Lett. 7 (2004) A408.
[24] F.Y. Zhang, X.G. Yang, C.Y. Wang, J. Electrochem. Soc. 153 (2) (2006) A225.
[25] C.Y. Wang, Chem. Rev. 104 (2004) 4727.
[26] X. Liu, H. Guo, C. Ma, J. Power Sources 156 (2006) 267.
[27] G. Karimi, X. Li, J. Power Sources 140 (2005) 1.
[28] K.H. Choi, D.H. Peck, C.S. Kim, D.R. Shin, T.H. Lee, J. Power Sources 86 (2000) 197.
[29] P. Argyropoulos, K. Scott, W.M. Taama, J. Chem. Eng. 73 (1999) 217.
[30] P. Argyropoulos, K. Scott, W.M. Taama, J. Chem. Eng. 73 (1999) 229.
[31] H. Yang, T.S. Zhao, Q. Ye, J. Power Sources 142 (2005) 117.
[32] S. Maharudrayya, S. Jayanti, A.P. Deshpande, J. Power Sources 157 (2006) 358.
[33] T.E. Springer, M.S. Wilson, S. Gottesfeld, J. Electrochem. Soc. 140 (12) (1993) 3513.